

Investigation of TiN Seed Layers for RABiTS Architectures With a Single-Crystal-Like Out-of-Plane Texture

C. Cantoni, A. Goyal, U. Schoop, X. Li, M. W. Rupich, C. Thieme, A. A. Gapud, T. Kodenkandath, T. Aytug, M. Paranthaman, K. Kim, J. D. Budai, and D. K. Christen

Abstract—Sharpening of the substrate texture is key to obtain critical current densities approaching single crystal values in coated conductors. In particular, great improvements in J_c are obtained by narrowing the substrate texture down to values of 3–4° for both phi-scan and omega-scan FWHM. The best Ni-alloy substrates used today for RABiTS show FWHM's of 6–5°. Although the majority of buffer layers deposited on these tapes by various techniques approximately duplicate the substrate's grain alignment, some materials have been found to develop much sharper out-of-plane texture. Here we report on growth and structural characterization of TiN seed layers on various textured metal tapes. TiN seed layers deposited by PLD have consistently shown tilting of the c -axis toward the direction of the sample's surface normal. We address the extent of such tilt and discuss feasibility of alternative RABiTS architectures that use a TiN seed layer to provide very sharp out-of-plane texture and serve as an effective metal-ion diffusion barrier.

Index Terms—Buffer layers for coated conductors, critical current density, epitaxial layers on textured metals, Ni-alloys, TiN, XRD texture.

I. INTRODUCTION

IN RABiTS [1] conductors the texture of the $\text{YBa}_2\text{Cu}_3\text{O}_{7-\delta}$ (YBCO) layer is closely related to the texture of the metal substrate because it results from epitaxial deposition of superconductor and underlying buffer layers on the $\{001\}\langle 100 \rangle$ cubic textured metal. Improvements in the out-of-plane texture of the buffer layers as compared to that of the metal substrate have often been reported, while no appreciable sharpening has been observed for the in-plane texture of films with respect to substrate [2]. As a consequence of the usually large lattice mismatch with the substrate (>6%), the buffer layers nucleate developing islands, which then coalesce with consequent formation of a sub-grain structure within each substrate grain. In this system, overgrowth of substrate grain boundaries by the buffer layer grains is highly unlikely and the in-plane orienta-

tion of the buffer layer is predominantly determined for each island at the time of nucleation. On the other hand, a change in the out-of-plane texture of the film (tilting of the $(00l)$ film planes with respect to the $(00l)$ substrate planes), is possible in low- and high-misfit systems as a consequence of growth on the vicinal metal surface [3]. Although still poorly understood, the phenomenon of tilted film growth on vicinal surfaces has been known since the beginning of semiconductor heteroepitaxy [4], [5]. The origin of such c -axis tilt is generally two-fold. In the first stage of deposition, below the critical thickness, the growth is pseudomorphic and strain energy accumulates in the film. In this system, as proposed originally by Nagai [4], the lattice constant of the film in the growth direction relaxes from the value a_s (lattice constant of the substrate) to the film value a_f over the length of a terrace introducing a tilt $\Delta\psi$ given by

$$\Delta\psi = \tan^{-1} \left(\frac{a_s - a_f}{a_s} \tan \psi \right),$$

where ψ is the miscut or vicinal angle. In this model the tilt will be away from the surface normal in the case $a_f > a_s$ and toward the surface normal if $a_f < a_s$. At some critical thickness misfit dislocations are introduced to relieve the mismatch strain, with consequent significant changes in the structure and energy of the growing film. Misfit dislocations with a component b_\perp of the Burgers vector normal to the interface can induce tilting, and, if the linear density of dislocations is sufficient to relieve the misfit $f = (a_f - a_s)/a_f$, the film tilt will be [5] $\Delta\psi = f \cdot b_\perp / b_\parallel$, where b_\parallel is the component of the Burgers vector parallel to the plane of the film. In an extended version of this model, Ayers *et al.* [6] have shown that the unequal distribution of certain misfit dislocations induced by the substrate miscut generates tilts toward the surface normal when $a_f > a_s$, opposite to the tilt direction in pseudomorphic systems. For buffer layers usually used in RABiTS, such as CeO_2 or Y_2O_3 , the observed sharpening of the (002) rocking curves is in the range of 1–2°. In this case the tilt is attributed to the coherent Nagai mechanism because the film monolayer d spacing is smaller than that of the Ni substrate [7]. In this paper we report on an alternative seed layer, TiN ($a_f < a_s$), which consistently shows larger rocking curve sharpening than those obtained by conventional buffer layers. We also show that the deposition of two additional layers, MgO and LaMnO_3 (LMO) on the TiN seed offers a robust alternative buffer layer architecture that can be used on highly reactive, Cr-containing, non magnetic substrates.

Manuscript received October 5, 2001. This work was sponsored by the U.S. Department of Energy under contract DE-AC05-00OR22725 with the Oak Ridge National Laboratory, managed by UT-Battelle, LLC.

C. Cantoni, A. Goyal, A. A. Gapud, T. Aytug, M. Paranthaman, J. D. Budai, and D. K. Christen are with the Oak Ridge National Laboratory, Oak Ridge, TN 37831, USA (e-mail: cantonic@ornl.gov).

U. Schoop, X. Li, M. W. Rupich, C. Thieme, and T. Kodenkandath are with the American Superconductor Corporation, Westborough, MA 01581, USA (e-mail: uschoop@amsuper.com).

K. Kim is with ORNL and the University of Florida, Gainesville, FL 32611, USA (e-mail: kyz@ornl.gov).

Digital Object Identifier 10.1109/TASC.2005.848691

II. EXPERIMENTAL

TiN films were grown by pulsed laser deposition (PLD) from a sintered TiN target on cube textured substrates of pure Cu, Ni-3%W, Ni-5%W, Ni-10%Cr-2%W, and Cu-48%Ni-1%Al. The deposition temperature varied depending on the substrate used and ranged between 580°C and 780°C. The background gas consisted of pure N₂ at a partial pressure of 8×10^{-4} Torr, the wavelength of the KrF excimer laser was 248 nm, and the beam energy per laser pulse was set to 280 mJ. The laser repetition rate used was 10 or 15 Hz and the film thickness was varied between 50 nm and 600 nm.

Analysis of film morphology by atomic force microscopy (AFM) revealed an average grain size of 20 nm for a 200 nm-thick film and a roughness of 0.4 nm measured on a $1 \mu\text{m} \times 1 \mu\text{m}$ area. X-ray diffraction (XRD) analysis showed that the TiN films were completely (00l) oriented, domains with orientation other than cube-on-cube were absent, and the percentage of cube textured material, as deduced by pole figures of the (111) reflection, was the same as for the metal substrate. The TiN (002) rocking curves measured both in the rolling and transverse direction exhibited a considerably smaller FWHM than that of the substrate.

To complete the buffer layer architecture MgO and LMO films were subsequently deposited *in situ* on the TiN films. For the deposition of the MgO layer the substrate temperature was lowered to 500°C, the N₂ evacuated and an O₂ flow established with a partial pressure of 1.0×10^{-5} Torr. MgO was then deposited by ablating an oxide target with a repetition rate of 10 to 15 Hz. For the deposition of the LMO layer the substrate temperature was raised to 700°C and the oxygen partial pressure was increased to 1.0×10^{-4} Torr. The repetition rate was 10 Hz and the beam energy was kept constant for all layers. The film thickness ranged from 80 nm to 150 nm for MgO and 100 nm to 200 nm for LMO.

III. DISCUSSION

There are two reasons for choosing MgO as second buffer layer. First, in the presence of oxygen, and at temperatures above 400°C, TiN has a high tendency to decompose to N₂ gas and TiO. This process hinders the epitaxial deposition of an oxide layer on TiN, unless the oxide to be deposited is thermodynamically more stable than TiO. MgO is one of few oxides to have a free energy of formation lower than that of TiO ($\Delta G_f^\circ[\text{MgO}] = -249 \text{ kcal/mole O}_2$; $\Delta G_f^\circ[\text{TiO}] = -213 \text{ kcal/mole O}_2$ at $T = 500^\circ\text{C}$). Therefore, MgO can be deposited at temperatures and oxygen pressures low enough to avoid formation of TiO on the TiN film surface. Secondly, MgO is structurally compatible with TiN, having the same rock-salt crystal structure and a lattice constant that is only 0.5% smaller. Finally, LMO is used as cap layer for its good structural compatibility with YBCO and the ease of epitaxial growth on MgO [8]. All samples selected for this study were scrutinized using XRD to insure that all layers consisted of only (002) cube-on-cube oriented domains.

Fig. 1 shows two graphs of the FWHM values for the (002) rocking curve of TiN films grown at various temperatures and with different thicknesses on Ni-3%W, Ni-5%W, Ni-10%Cr-2%W, Cu and Cu-48%Ni-1%Al substrates. The data is plotted

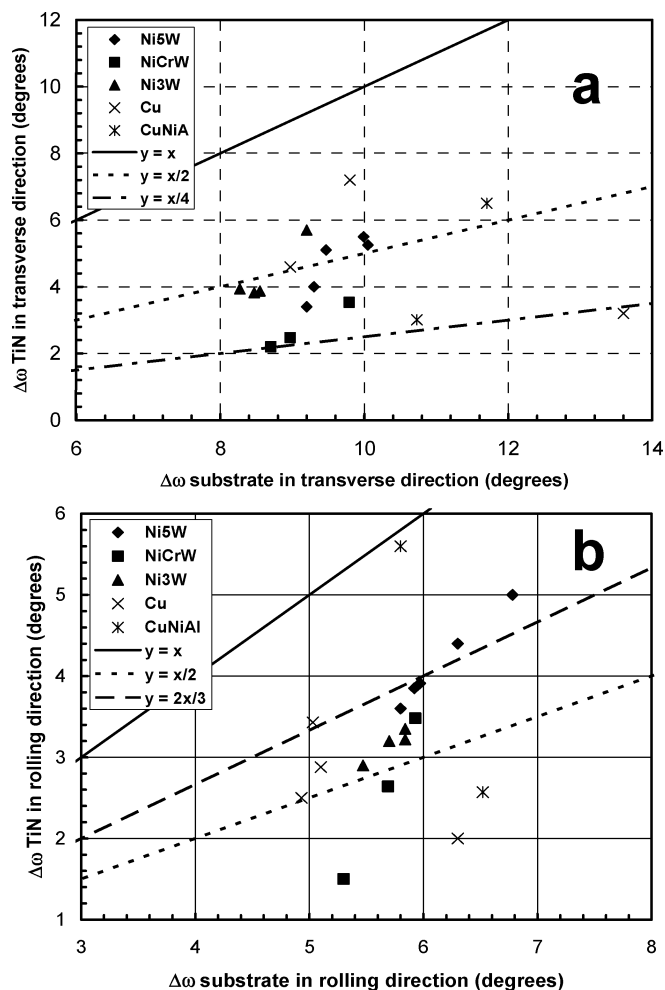


Fig. 1. FWHM's of the TiN (002) rocking curves versus corresponding FWHM's of the (002) substrate rocking curve, for TiN films on different textured substrates. The rocking curves are acquired in the rolling direction (a), and in the transverse direction (b).

against the corresponding FWHM values of the substrate (002) rocking curves. In Fig. 1(a) the FWHM's of films and substrates are measured with azimuth parallel to the transverse direction of the tape, and in Fig. 1(b) the azimuth is parallel to the rolling direction. In both cases the FWHM values for the TiN films are considerably smaller than the corresponding values for the substrate. The rocking curve sharpening is more evident in the transverse direction where the majority of the films exhibit a FWHM ranging between 1/2 and 1/4 of the substrate value. Particularly impressive is the case of one of the TiN films on Cu for which the transverse FWHM improved by 10.4° , from a value of 13.6° in the substrate to a value of 3.2° in the film. For the same film the corresponding FWHM values in the rolling direction were 6.3° and 2° .

Fig. 2 shows a comparison between grain boundary (GB) maps obtained by electron backscattering Kikuchi patterns (EBKP) from a biaxially textured Cu substrate and a TiN film deposited on the same substrate. Fig. 2(a) is acquired on the TiN film and highlights only GB's with a total misorientation larger than 3° . It is clear that with this criterion, macroscopic percolation of current is possible and most of the material is connected by GB's $\leq 3^\circ$. If the same criterion is used for the

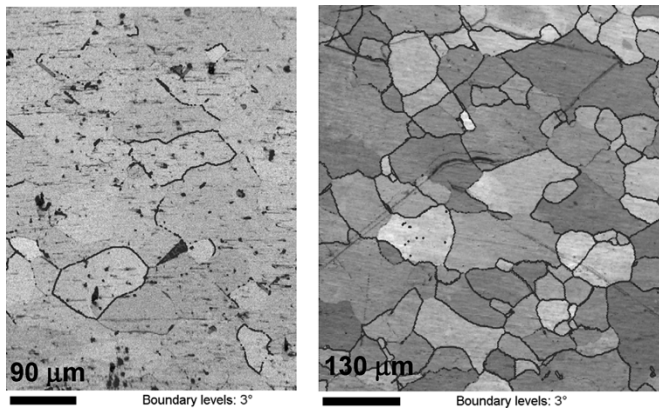


Fig. 2. EBKP maps showing grain boundaries larger than 3° of a TiN film on Cu (a), and the underlying Cu substrate (b).

Cu substrate (Fig. 2(b)), the distribution of highlighted GB's becomes much denser and current percolation through GB's $\leq 3^\circ$ is not possible. To obtain in the substrate a fraction of connected grains similar to that shown by the TiN film, we have to raise the criterion to an angle of 7° . In other words, if buffers and superconductor were to replicate faithfully the texture of the substrate, macroscopic current percolation would occur by transport through GB's of angle $\leq 7^\circ$. The EBKP maps clearly show that the GB distribution has shifted toward much lower angles in the TiN film as compared to the substrate. However, in these maps no distinction is made between GB's obtained by tilt about the c-axis or an in-plane axis. At this point it is not clear whether GB's formed by in-plane or out-of-plane misorientations have similar effects on the critical current density, and it has been suggested that, for GB angles of 5° – 7° , pure out-of-plane misorientations have a smaller effect on the superconducting transport properties than in-plane misorientations [9].

Comparison of XRD ϕ -scans of the (111) reflections in TiN films and metal substrates have shown that when the (111) peak FWHM is corrected for the broadening caused by the out-of-plane spread $\Delta\omega$ and the X angle of the particular reflection chosen, the resulting "true" $\Delta\phi$ [10] is the same for film and substrate. Therefore, in principle, a buffer layer architecture that uses TiN as a seed layer offers the possibility of investigating uniquely the effect of the out-of-plane texture on J_c . However, before any speculation on the role of the out-of-plane texture can be made, the ability of the buffer layer architecture to block or sufficiently inhibit metal and oxygen diffusion and support high J_c YBCO films needs to be addressed. We tested the robustness of our LMO/MgO/TiN architecture by depositing the YBCO layer by an industrial, well established, and high performance method such as the American Superconductor Corporation (AMSC) metal-organic deposition (MOD) YBCO process [11].

A sputtered CeO_2 cap layer was first deposited by AMSC on our architecture for chemically compatibility with the ex situ YBCO process. Subsequently, the superconductor precursor was deposited and processed to obtain an YBCO film of $0.8 \mu\text{m}$ in thickness. Two different substrates were used for this experiment: Ni-5%W and a Ni-10%Cr-2%W alloy; both provided by AMSC. In particular, in the Ni-10%Cr-2%W substrate,

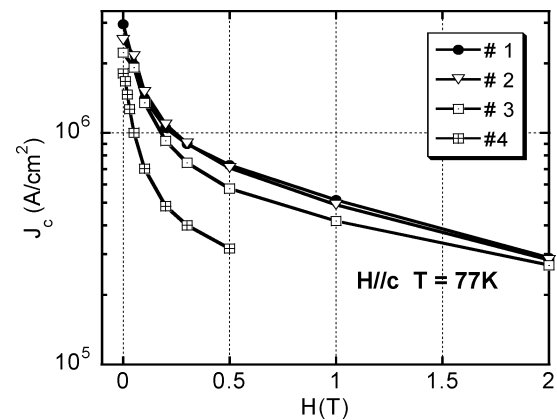


Fig. 3. Comparison of $J_c(H)$ curves at 77 K and $H//c$ for the 4 samples in Table I having different out-of-plane texture but similar in-plane texture.

magnetism is completely suppressed down to 4 K [12]. For this reason, fabrication of Ni-10%Cr-2%W-based RABiTS conductors is extremely interesting in view of applications that require minimization of ac losses. Unfortunately, Cr-containing alloys are extremely reactive toward oxygen and deposition of oriented oxide buffer layers on these substrates has not been possible. TiN offers the advantage of deposition in an oxygen-free environment and can be nucleated on Ni-10%Cr-2%W once the native metal oxide layer on the surface of the alloy is removed in situ, typically by Ar^+ ion sputtering. In both cases the YBCO was fully (00 l) oriented and showed a considerably sharper out-of-plane texture as compared to that of the substrate. For the YBCO on the Ni-10%Cr-2%W substrate, the rocking curves of the (005) peak showed a sharpening of 2.5° and 5.9° for the rolling and transverse directions, respectively. For the YBCO film on the Ni-5%W substrate the (005) rocking curves were 1.1° sharper in the rolling direction and 4.9° sharper in the transverse direction as compared to the substrate values. The transport critical current density in self-field at 77 K was 1.8 MA/cm^2 for the Ni-10%Cr-2%W sample and 2 MA/cm^2 for the sample on Ni-5%W, comparable to average J_c values obtained by AMSC on their $\text{Y}_2\text{O}_3/\text{YSZ}/\text{CeO}_2$ buffered substrates. Such a high J_c on very reactive metal substrates is a clear indication that the buffer layers perform well as diffusion barriers and have good chemical and structural properties.

To investigate the effect of out-of-plane sharpening on J_c we used samples on which YBCO films of thickness $0.2 \mu\text{m}$ were grown by PLD. The quality of PLD YBCO films is in fact much less dependent on the type of cap layer used as compared to ex situ processed YBCO films, and high- J_c films are routinely deposited on perovskite buffer layers such as LMO and $\text{La}_{0.7}\text{Sr}_{0.3}\text{MnO}_3$ (LSMO) [13].

Fig. 3 shows a comparison between $J_c(H)$ curves obtained at 77 K from $0.2\text{-}\mu\text{m}$ -thick YBCO films deposited in the same PLD conditions (using the same PLD chamber and YBCO target) on substrates with comparable in-plane texture but significantly different out-of-plane texture. Although the samples architectures are different, Fig. 3 compares samples with optimal performance to minimize the role of possible defects in the buffer layers. Table I shows the FWHM of YBCO $\Delta\omega$ and $\Delta\phi$ scans for the samples in Fig. 3 and their architectures.

TABLE I
BUFFER LAYER ARCHITECTURE AND FWHM FOR $\Delta\omega$ AND $\Delta\phi$ SCANS
FOR THE SAMPLES SHOWN IN FIG. 3 ALONG THE ROLLING (R) AND
TRANSVERSE (T) DIRECTIONS

#	ARCHITECTURE	YBCO $\Delta\omega$, R ($^\circ$)	YBCO $\Delta\omega$, T ($^\circ$)	YBCO $\Delta\phi$ ($^\circ$)
1	LMO/MgO/TiN/Ni3W	3.1	4.1	7.5
2	CeO ₂ /LMO/MgO/TiN/ Ni3W	6.3	7.5	7.9
3	LSMO/ir/Ni3W	4.7	--	7.2
4	CeO ₂ /YSZ/Y ₂ O ₃ /Ni5W	6.6	5.8	6.4

As shown in Fig. 3, sample # 1, with a TiN seed layer and the sharpest out-of-plane texture, has the highest self-field J_c . Samples # 3 and # 4 show lower J_c than sample # 1, with sample # 4 having the largest $\Delta\omega$ in the rolling direction, and also the lowest J_c at all fields. We note that sample # 3 and # 4 have buffer architectures very different from sample # 1 and may not constitute optimal control samples. Sample # 2 is our best choice for comparison with sample # 1. Samples # 1 and # 2 have in fact the same architecture except for a thin CeO₂ cap used in sample # 2. The significantly broader out-of-plane texture of sample # 2 is due to a broader metal substrate out-of-plane texture and different deposition conditions for the LMO layer, which led to broader rocking curves for this layer as compared to those of MgO and TiN. The CeO₂ texture then replicated that of the LMO layer. Interestingly, these two samples show very comparable J_c . These findings suggest that more work is necessary to assess the role of out-of-plane texture in RABiTS. While the in-field J_c values for samples # 1, # 2, and # 3 are comparable, the performance of sample # 4 in field is significantly lower. This suggests that the difference in J_c between sample # 4 and sample # 1 is caused by reasons other than texture and may reflect a difference in the intra-grain J_c of the two samples. This study shows that a sharpening up to 3° in the out-of-plane texture does not dramatically increase the critical current capability of RABiTS.

IV. CONCLUSION

We presented an alternative RABiTS architecture consisting of LMO/MgO/TiN deposited by PLD. Such architecture meets the buffer layer requirements for coated conductors and can sustain high J_c in YBCO films processed by MOD on highly reac-

tive nonmagnetic substrates. In addition, due to a tilted epitaxy growth mechanism in the TiN seed, considerable sharpening of the out-of-plane texture occurs in YBCO films deposited on such architecture. However, our preliminary comparative results suggest that a reduction of $\Delta\omega$ from values of $6\text{--}7^\circ$ to values of $3\text{--}4^\circ$ does not considerably increase the critical current density at 77 K.

REFERENCES

- [1] D. P. Norton *et al.*, "Epitaxial YBa₂Cu₃O₇ on biaxially textured nickel (001): an approach to superconducting tapes with high critical current density," *Science*, vol. 274(5288), pp. 755–757, Nov. 1996.
- [2] Q. He, D. K. Christen, J. D. Budai, E. D. Specht, D. F. Lee, A. Goyal, D. P. Norton, M. Paranthaman, F. A. List, and D. M. Kroeger, "Deposition of biaxially-oriented metal and oxide buffer-layer films on textured Ni tapes: new substrates for high-current, high-temperature superconductors," *Physica C*, vol. 275, pp. 155–161, 1997.
- [3] F. Riesz, "Crystallographic tilting in high-misfit (100) semiconductor heteroepitaxial systems," *J. Vac. Sci. Technol. A*, vol. 14(2), pp. 425–430, 1996.
- [4] H. Nagai, "Structure of vapor-deposited GaxIn1-xAs crystals," *J. Appl. Phys.*, vol. 45, pp. 3789–3794, Sep. 1974.
- [5] G. H. Olsen and R. T. Smith, "Misorientation and tetragonal distortion in heteroepitaxial vapor-grown III-V Structures," *Phys. Stat. Sol. A*, vol. 31, pp. 739–747, 1975.
- [6] J. E. Ayers, S. K. Ghandhi, and L. J. Schowalter, "Crystallographic tilting of heteroepitaxial layers," *Journal of Crystal Growth*, vol. 113, pp. 430–440, 1991.
- [7] J. Budai *et al.*, "X-ray microdiffraction study of growth modes and crystallographic tilts in oxide films on metal substrates," *Nature Materials*, vol. 2, pp. 487–492, Jul. 2003.
- [8] M. Paranthaman *et al.*, "Growth of thick YBa₂Cu₃O_{7- δ} films carrying a critical current density of 230 A/cm on single LaMnO₃-buffered ion-beam assisted deposition MgO substrates," *J. Mater. Res.*, vol. 18, p. 2055, 2003.
- [9] A. Goyal. RABiTS-based strategic research. presented at the DOE Peer Review on Superconductivity. [Online] Available: http://www.ornl.gov/sci/htsc/documents/pdf/fy2004/RABiTS-Based_Strategic_Research.pdf.
- [10] ———, RABiTS substrates research and development. presented at the DOE Peer Review on Superconductivity. [Online] Available: http://www.ornl.gov/sci/htsc/documents/pdf/fy2003/RABiTS_Substrates_R&D-Goyal.pdf
- [11] A. Malozemoff. Second Generation HTS Wire: An Assessment. [Online] Available: http://www.amsuper.com/products/htsWire/documents/4122GWhitePaper_v5.pdf
- [12] Ref. 8 and J. R. Thompson, "Private Communication," unpublished (e-mail: jrt@utk.edu).
- [13] T. Aytug *et al.*, "An approach for electrical self-stabilization of high-temperature superconducting wires for power application," *Appl. Phys. Lett.* in press.